Long jumps in the strong-collision model

R. Ferrando,* F. Montalenti, R. Spadacini, and G.E. Tommei
INFM and CFSBT/CNR, Dipartimento di Fisica dell' Università di Genova, via Dodecaneso 33, 16146 Genova, Italy
(Received 14 September 1999; revised manuscript received 14 February 2000)

The jump-length probability distribution for a classical particle diffusing in a periodic potential is calculated in the framework of a strong-collision model, where each collision of the particle with the thermal bath reequilibrates the velocity. Exact numerical results are obtained by the matrix-continued-fraction method, and two different analytical approximations are developed. In the first approximations it is assumed that an activated particle is always retrapped in the cell where it suffers the first collision; in the second approximation it is assumed that only the collisions giving a final total energy which is lower than the activation barrier are effective for retrapping. This second analytical approximation is in excellent agreement with the numerical data.

PACS number(s): 05.40.−a, 05.60.−k, 68.35.Fx

I. INTRODUCTION

The diffusion of classical particles in periodic potentials is a topic of great interest in many fields of physics, chemistry, and biology [1–4]. In the most popular model, diffusion is treated as a Brownian motion, which can be described by means of some form of the Langevin (or of the Fokker-Planck) equation [2]. In the simplest Langevin equation, the particle is coupled to the environment by a friction η and by a white noise, which are related to each other by the fluctuation-dissipation theorem. In this model, at low friction, the particle changes its energy gradually, by suffering many weak collisions with the heat bath. The velocity of the particle is slightly modified by a single collision, and thermalization occurs because of the large number of those collisions.

On the other hand, it may happen that the particle interacts with the heat bath by strong and well-separated collisions, moving in a deterministic way in between. In this case, the key point is the determination of the effect of one collision on the particle motion. A reasonably simple approximation is to assume that after each collision the velocity of the particle is suddenly thermalized, i.e., after a collision the final velocity is extracted from the Maxwell distribution at the given temperature T. This gives rise to the Bhatnagar, Gross, and Krook (BGK) [5,1] kinetic equation for the probability density in phase space $f(x,v,t)$:

$$\frac{\partial f}{\partial t}+v\frac{\partial f}{\partial x}+\frac{F(x)}{m}\frac{\partial f}{\partial v}=\eta\left[M(v)\int_{-\infty}^{+\infty}f(x,v,t)dv-f(x,v,t)\right], \tag{1}$$

where η is the collision frequency, $F(x)$ is the periodic force coming from the potential $U(x)$, m is the mass of the particle, and $M(v)$ is the Maxwell distribution

$$M(v)=\left(\frac{m}{2\pi k_B T}\right)^{1/2}\exp\left(-\frac{mv^2}{2k_B T}\right). \tag{2}$$

Equation (1) can be derived also along the lines developed in Ref. [6] by making the above assumption on the effect of particle-bath collisions. A strong collision model, where the effect of each collision is to thermalize not only the velocity (as strictly required in the BGK model) but also the position of the particle, has been recently studied by Bicout et al. [7].

The BGK model can be proposed for the description of the classical diffusion of atoms or molecules in periodic systems (like in the case of adatoms on surfaces or in zeolites [6]) in the cases in which the following physical assumptions are fulfilled.

(a) The energy exchange between the diffusing particle and the thermal bath can be modeled by well separated collisions.

(b) Each of these collisions leads to a quite strong energy exchange, of the order of $k_B T$.

Neither (a) nor (b) can be justified rigorously from a microscopic point of view; however, these assumptions can be considered reasonable approximations when the vibrational period of the diffusing particle in the well is much shorter than the typical inverse frequencies of the substrate phonons [6]. Roughly speaking, the latter condition is likely to be fulfilled when the mass of the adparticle is much smaller than the mass of the substrate atoms. On the other hand, the white-noise Langevin approach [8–10] is valid in the opposite conditions, i.e., when the characteristic vibrational times of the adparticle are slower than those of the substrate. This happens usually when the adsorbate has a larger mass or the same mass as the substrate atoms [11]; even in the case of light adsorbates the time-scale condition leading to the Langevin approximation can be fulfilled [9]. However, we remark that the differences between the Langevin and the BGK approaches are significant only at intermediate and small η, since the two equations tend to the same limit (the Smoluchowski equation) for $\eta\to\infty$ [1].

When a particle moves in a periodic potential, different diffusion mechanisms are possible, depending on the barrier height (compared to the thermal energy $k_B T$) and on the

*Author to whom correspondence should be addressed. Electronic address: ferrando@fisica.unige.it

strength of the coupling between the particle and the thermal bath (in our case, depending on the collision frequency η). If the barrier is sufficiently high, the particle spends the most part of the time by making small-amplitude oscillations around the well bottoms, and sometimes is activated and makes a jump from a well to another (jump diffusion). This happens when the barrier E_A is larger of about $4\,k_BT$ [8]. Once the particle has escaped a well, it may be retrapped in a nearest-neighbor one (thus making a single jump) or it may make a flight after which is captured in a cell which is far away from the cell of departure (in this case making what we shall call a long jump). Long jumps in surface diffusion recently attracted noticeable interest both from the experimental and the theoretical point of views. In fact, experiments in the field of surface diffusion have shown that adsorbed atoms can make a rather large percentage of long jumps in systems like Pd/W(211) [12] and Pt/Pt(110) [13]. From a theoretical point of view, many investigations about long jumps have been carried out in the framework of the Langevin (Fokker-Planck) model [14,15,8–10,16–18]. Here, we develop a theory of long jumps on the basis of the BGK kinetic model (Eq.(1)). Our approach is similar to the one by Beenakker and Krylov (BK) in Ref. [19]. In their treatment, BK considered a particle with an energy k_BT above the maximum U_M of the potential $U(x)$ (an *unbound* particle in BK terminology). They assumed that any collision of an unbound particle with the thermal bath (phonons) leads to retrapping (thus becoming a *bound* particle), neglecting the role of unbound-unbound transitions, and they calculated the jump-length probability distribution (JLPD). In our treatment [i.e., in Eq. (1)], we do not separate unbound-bound transitions from unbound-unbound transitions, but we assume that the effect of *any* collision is to reequilibrate the velocity distribution.

In the following, we calculate the JLPD for the model of Eq. (1) by two different methods. The first method is numerical. It is based on the solution of the kinetic equation by the matrix-continued-fraction method (MCFM) [1], which allows the calculation of the dynamic structure factor $S_s(q,\omega)$. From S_s, the JLPD is extracted by making a Fourier analysis of the energy width of the quasielastic peak [8]. This numerical method gives exact results, but it can be applied only in limited ranges of barriers and collision frequencies. In fact, it becomes very computationally demanding at high barriers and/or low collision frequencies. In some cases, the direct simulation of the model by means of molecular-dynamics techniques (see the following) could be more convenient. However, also the direct simulation suffers from the same drawbacks as the MCFM solution. For the above reasons, in the following we develop analytical approximations and test their reliability against the exact numerical results. In particular we show that it is possible to build up a rather simple analytical treatment which gives very accurate results.

The paper is structured as follows. In Sec. II we describe the numerical method of solution. In Sec. III we develop the analytical treatment and in Sec. IV we compare numerical and analytical results. Section V contains the conclusions.

II. NUMERICAL METHOD

As said in the introduction, a reliable numerical method for calculating the JLPD is based on the Fourier analysis of the decay function $f(q)$ which coincides, in the jump-diffusion regime, with the half-width (in frequency) of the quasielastic peak of the dynamic structure factor $S_s(q,\omega)$ [8]. In the following, we give only a brief summary of the method. The details can be found in Refs. [1,8,20]. $S_s(q,\omega)$ can be calculated via a matrix-continued-fraction expansion [1]. $S_s(q,\omega)$ is defined by

$$S_s(q,\omega)=\frac{1}{2\pi}\int_{-\infty}^{+\infty}\langle\exp\{iq[x(t)-x(0)]\}\rangle\exp(-i\omega t)dt. \tag{3}$$

In order to calculate the characteristic function in the integral the computation of the conditional probability $P_c(x,v,t/x_0,v_0,0)$ is needed. The latter is the solution of Eq. (1) with the initial condition $P_c(x,v,0/x_0,v_0,0)=\delta(x-x_0)\delta(v-v_0)$. P_c is then expanded on an orthonormal basis, with the aid of Bloch's theorem for the spatial part and in Hermite functions in the velocity part. The decay function $f(q)$ is recovered from $S_s(q,\omega)$ by the following limit [8]:

$$f(q)=\lim_{\omega\to 0}\omega\left[\frac{S_s(q,\omega)}{S_s(q,0)}-1\right]^{1/2}. \tag{4}$$

The JLPD follows from the Fourier analysis of $f(q)$; specifically the probability $P(n)$ of a jump of length n is given by

$$P(n)=-\frac{2a}{\pi r_j}\int_0^{\pi/a}f(q)\cos(naq)dq, \tag{5}$$

where the jump rate r_j is obtained as

$$r_j=\frac{a}{\pi}\int_0^{\pi/a}f(q)dq. \tag{6}$$

The results concerning the jump rate r_j were already shown in Ref. [21] and they will not be repeated here; in the following we focus on the jump-length distribution. After some algebra [1,20], it turns out that, in the first Brillouin zone, S_s is given by

$$S_s(q,\omega)=N\,\mathrm{Re}\left\{\sum_{p,r=-\infty}^{\infty}\tilde{G}^{pr}(k,i\Omega)M_pM_r^*\right\}, \tag{7}$$

where $\Omega=(a/2\pi)(m/k_BT)^{1/2}\omega$, $q=2\pi k/a$, $|k|<1/2$, M_p is given by

$$M_p=\frac{1}{a}\int_{-a/2}^{a/2}dx\exp\left(-\frac{V(x)}{2k_BT}\right)\exp\left(\frac{2\pi px}{a}\right), \tag{8}$$

and N is a normalization factor. The Green function $\tilde{\mathbf{G}}$ is given by

$$\tilde{\mathbf{G}}(k,i\Omega)=[i\Omega\mathbf{I}+\mathbf{B}^+[(i\Omega+\gamma)\mathbf{I}+2\mathbf{B}^+[(i\Omega+\gamma)\mathbf{I}+\ldots]^{-1}\mathbf{B}^-]^{-1}\mathbf{B}^-]^{-1}. \tag{9}$$

In the above equation the normalized collision frequency γ is defined as

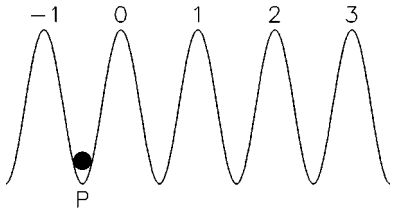

FIG. 1. Periodic potential $U(x)$; the particle starts from the cell around point P and then crosses the barriers in 0,1,2, ...

$$\gamma = \eta \frac{a}{2\pi}\sqrt{\frac{m}{k_B T}}, \tag{10}$$

I is the identity matrix and $\mathbf{B}^{\pm}$ are given, for an even potential, by

$$B^{\pm}_{pr}(k) = (p+k)\,\delta_{pr} \pm \frac{1}{4\pi}\int_{-\pi}^{+\pi} dx\, F(x)\sin[(r-p)x]. \tag{11}$$

The MCFM becomes very cumbersome at high barriers or at low friction. This is especially true in the BGK model, where the continued fraction converges much slower than in the Langevin (Fokker-Planck) case. In fact, even at $\gamma = 0.1$ more than 1000 iterations in Eq. (9) are necessary to obtain a good convergence, whereas in the Fokker-Planck case 200 iterations were sufficient to guarantee the same degree of numerical accuracy. Because of that, at $\gamma < 0.1$ it may be convenient to solve the BGK model by means of direct simulation (while the MCFM is more precise and convenient at higher friction). In the direct simulation the particle moves deterministically in the periodic field of force by the Newton equations of motion, until it suffers a collision. In fact, at each time step δt ($\delta t \ll \eta^{-1}$), the particle has a probability $\eta\delta t$ of experiencing a collision with the thermal bath. After the collision, the velocity of the particle is extracted randomly from the Maxwell distribution at the given temperature. This procedure essentially coincides with the one of the Andersen thermostat in canonical molecular-dynamics simulations (see for example [22]). We have used the direct simulation in order to check the MCFM results. All the results reported in the figures are, however, obtained by the MCFM method.

Finally, we remark that, even by direct simulation, it would be very difficult to accumulate a reasonable statistics of events at $\gamma < 10^{-3}$, because jumps become less frequent as γ decreases. Moreover, both numerical methods become practically useless at high barriers ($E_A > 20\,k_B T$), where analytical approaches are needed (both for Langevin, as already developed in [14,10,23] and for BGK, where an analytical formulation is still lacking). For this reason, we devote the following section to the development of accurate analytical expressions for the probability distribution of jump lengths in the BGK model.

III. ANALYTICAL SOLUTION FOR THE JUMP-LENGTH PROBABILITY DISTRIBUTION

Let us consider a particle in a periodic potential $U(x)$. The particle is initially at equilibrium in a lattice cell (near point P in Fig. 1) and then makes a jump (for example, to the right). Let E_0 be the initial kinetic energy at the crossing of the 0th saddle point (see Fig. 1), and take $t=0$ at the crossing of this saddle point. By definition,

$$E_0 = \frac{1}{2} m v_0^2. \tag{12}$$

The total energy at $t=0$ is E_{tot}

$$E_{tot} = U_M + E_0, \tag{13}$$

where U_M is the potential energy at saddle points. Let us define

$$\varepsilon = \frac{E_0}{k_B T}, \quad u(x) = \frac{U(x)}{k_B T}, \quad u_M = \frac{U_M}{k_B T}. \tag{14}$$

The probablity of suffering a collision during the time dt is $d\tilde{\mathcal{P}}$

$$d\tilde{\mathcal{P}} = \eta dt = \eta \frac{dx}{v(x,\varepsilon)}, \tag{15}$$

where

$$v(x,\varepsilon) = \sqrt{\frac{2k_B T}{m}[\varepsilon + u_M - u(x)]}. \tag{16}$$

Now, we can proceed according to two different approximation schemes. In the first case, we assume that all collisions are effective, in the sense that the particle is always trapped in the cell where it suffers its first collision. This approximation is analogous to the one by BK [19] and *overestimates* the probability of single jumps. In this case, the probability of not being trapped up to the nth saddle point (which is at distance $x = na$ and it is crossed at time t_n) is

$$\tilde{Q}(n,\varepsilon) = \exp(-\eta t_n) = \exp\left(-\eta \int_0^{na} \frac{dx}{v(x,\varepsilon)}\right)$$
$$= \exp[-n\tilde{\varphi}(\varepsilon)], \tag{17}$$

where

$$\tilde{\varphi}(\varepsilon) = \eta \int_0^a \frac{dx}{v(x,\varepsilon)}. \tag{18}$$

The probability of being trapped in the nth cell is then

$$\tilde{P}(n,\varepsilon) = \tilde{Q}(n-1,\varepsilon) - \tilde{Q}(n,\varepsilon). \tag{19}$$

Now we have to average over the initial energy distribution, which is exponential (as checked by direct simulation), and find

$$\tilde{P}(n) = \langle \tilde{P}(n,\varepsilon)\rangle = \int_0^\infty d\varepsilon \exp(-\varepsilon)\tilde{P}(n,\varepsilon). \tag{20}$$

Now we average the arguments of the exponentials instead of averaging the exponentials themselves:

$$\tilde{P}(n)=\langle \exp[-(n-1)\tilde{\varphi}(\varepsilon)]-\exp[-n\tilde{\varphi}(\varepsilon)]\rangle$$
$$\simeq \exp(-(n-1)\tilde{\varphi})-\exp(-n\tilde{\varphi}), \quad (21)$$

where

$$\tilde{\varphi}=\langle \tilde{\varphi}(\varepsilon)\rangle. \quad (22)$$

The exchange between the average and the exponential does not introduce any significant difference in the results. Indeed, except for a weak logarithmic divergence at $\varepsilon\to 0$, $\tilde{\varphi}(\varepsilon)$ varies much more slowly than ε [in fact, at large ε, $\tilde{\varphi}(\varepsilon)\sim\varepsilon^{-1/2}$]; if $\tilde{\varphi}(\varepsilon)$ would have been a constant, the exchange between the average and the exponential would have been exact. However, one can retain the average outside of the exponentials and use the second member of Eq. (21) to compute $\tilde{P}(n)$, instead of the third member. This is simply a little bit more expensive from a computational point of view (however, much less expensive than MCFM or direct simulation), but we have checked that it does not introduce any significant change in the results in the parameter range that we consider in the following. The same considerations apply also to the derivation of $P^*(n)$ (see the following).

Explicitly, the formula for $\tilde{\varphi}$ is

$$\tilde{\varphi}=\eta\sqrt{\frac{m}{2k_BT}}\int_0^\infty d\varepsilon \exp(-\varepsilon)\int_0^a \frac{dx}{\sqrt{\varepsilon+u_M-u(x)}}. \quad (23)$$

A second approximation scheme relies on the assumption that only the collisions in which the final energy is below U_M are effective. In this case, the particle is not trapped always in the cell where it experiences its first collision, but it is trapped there only if the collision is effective, i.e., if its final velocity v_f after that collision (experienced at point x) satisfies

$$\frac{1}{2}mv_f^2+U(x)\leqslant U_M. \quad (24)$$

This gives an effective collision frequency $\eta_{eff}(x)$

$$\eta_{eff}(x)=2\eta\int_0^{\sqrt{(2k_BT/m)[u_M-u(x)]}} M(v)dv$$
$$=\eta\,\mathrm{erf}[\sqrt{u_M-u(x)}], \quad (25)$$

where $M(v)$ is the Maxwell equilibrium distribution, and

$$\mathrm{erf}(x)=\frac{2}{\sqrt{\pi}}\int_0^x dt\,\exp(-t^2). \quad (26)$$

The probability of suffering an effective collision is thus

$$d\mathcal{P}^*=\eta_{eff}(x)\frac{dx}{v(x,\varepsilon)}=\eta\,\mathrm{erf}[\sqrt{u_M-u(x)}]\frac{dx}{v(x,\varepsilon)}. \quad (27)$$

Following the same lines as before, we find

$$P^*(n)=\exp[-(n-1)\varphi^*]-\exp(-n\varphi^*) \quad (28)$$

with

$$\varphi^*=\eta\sqrt{\frac{m}{2k_BT}}\int_0^\infty d\varepsilon\exp(-\varepsilon)\int_0^a dx\frac{\mathrm{erf}\,[\sqrt{u_M-u(x)}]}{\sqrt{\varepsilon+u_M-u(x)}}. \quad (29)$$

Equations (28) and (29) *underestimate* the probability of single jumps $P(1)$, since they assume that particles experiencing a noneffective collision proceed undisturbed as if they had not collided at all. We recall that Eqs. (21) and (23) lead to an *overestimate* of $P(1)$. As we shall show in the following by direct comparison with the numerical results, $P^*(n)$ is a much better approximation of $P(n)$ than $\tilde{P}(n)$.

IV. COMPARISON OF THE ANALYTICAL APPROXIMATIONS WITH THE NUMERICAL RESULTS

In the following we compare the analytical solutions of Sec. III with the exact numerical results from the Fourier analysis of the decay function $f(q)$ (see Sec. II) in the case of a cosine potential:

$$U(x)=A[1-\cos(x)], \quad (30)$$

having defined the parameter g

$$g=\frac{A}{2k_BT}=\frac{E_A}{4k_bT}, \quad (31)$$

($E_A=2A$ is the activation barrier) one has

$$\tilde{\varphi}=\frac{\gamma}{\sqrt{2}}\int_0^\infty d\varepsilon\exp(-\varepsilon)\int_0^{2\pi}\frac{dz}{\sqrt{\varepsilon+2g[1+\cos(z)]}}, \quad (32)$$

$$\varphi^*=\frac{\gamma}{\sqrt{2}}\int_0^\infty d\varepsilon\exp(-\varepsilon)\int_0^{2\pi}dz\frac{\mathrm{erf}\{\sqrt{2g[1+\cos(z)]}\}}{\sqrt{\varepsilon+2g[1+\cos(z)]}}, \quad (33)$$

with the normalized friction γ given by Eq. (10).

In Fig. 2 the behavior of $P(n)$ for $n=1,2,\ldots,8$ is reported as a function of γ at fixed activation barrier ($g=1.5$, $E_A=6\,k_BT$). The symbols correspond to the exact numerical results and the lines to the analytical approximation $P^*(n)$ of Eqs. (28) and (29). As expected, the single-jump probability $P(1)$ decreases with γ, because an increase of the collision frequency causes an easier retrapping. Moreover, each $P(n)$ for $n\geqslant 2$ has a maximum which is shifted to lower and lower γ at increasing n. This is analogous to what happens in the case of the Langevin (Fokker-Planck) model [8] and can be easily understood by noticing that the $P(n)$, $n\geqslant 2$ tend to 0 both at $\gamma\to\infty$ (retrapping is always in the first cell) and at $\gamma\to 0$ (retrapping tends to be equally likely in any cell).

Concerning the comparison of the analytical results with the numerical data, it is evident that the $P^*(n)$ are very accurate in a wide range of γ, and also for large n. On the other hand, the approximation $\tilde{P}(n)$ [Eqs. (21) and (23)] is less satisfactory, as can be seen in Fig. 3. There, the numerical results for $P(1)$ (black circles) and $P(2)$ (black squares) are compared to $P^*(1)$ (full line), $P^*(2)$ (dash-dotted line), $\tilde{P}(1)$ (dashed line), and $\tilde{P}(2)$ (dotted line).

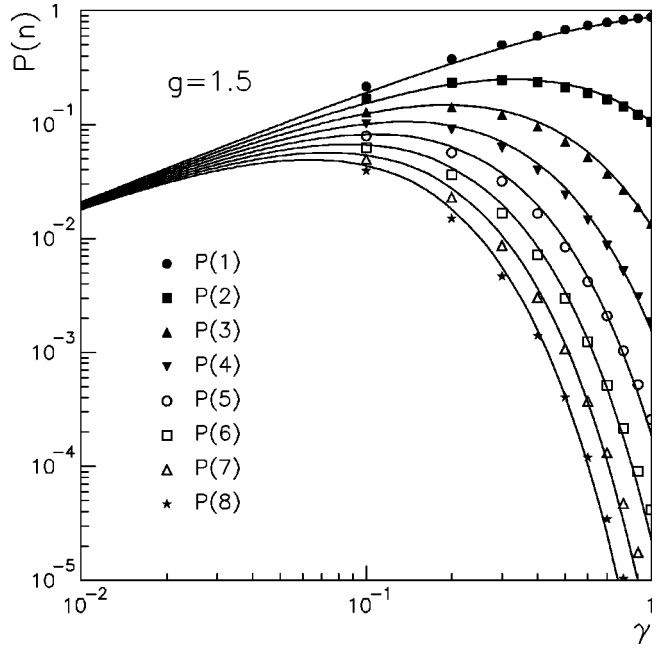

FIG. 2. Jump probabilities for lengths from one to eight cells. The symbols refer to the exact numerical results $[P(n)]$, whereas the full lines correspond to the analytical approximation $P^*(n)$. The error bars on the numerical points are smaller than the size of the dots.

As underlined in Sec. III, the numerical results lie always in between the two analytical approximations. However, they almost coincide with the P^*, especially at large γ. This shows that retrapping is not occurring at each collision; the retrapping frequency at a given point x is very well approximated by the effective collision frequency $\eta_{eff}(x)$ of Eq. (25).

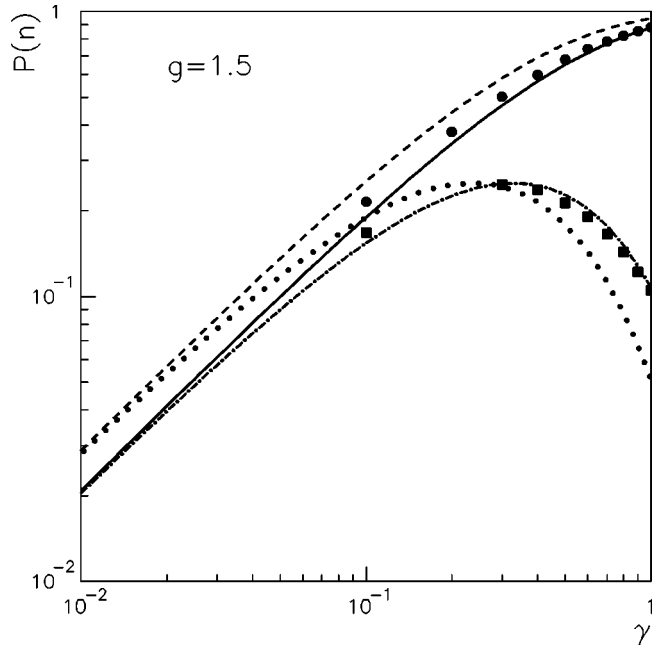

FIG. 3. Comparison of the analytical approximations $P^*(n)$ and $\tilde{P}(n)$ with the exact numerical results $P(n)$ for $n=1$ and 2. The black circles correspond to $P(1)$, the full line to $P^*(1)$, and the dashed line to $\tilde{P}(1)$; the black squares correspond to $P(2)$, and the dash-dotted line to $P^*(2)$, and the dotted line to $\tilde{P}(2)$. The error bars on the numerical points are smaller than the size of the dots.

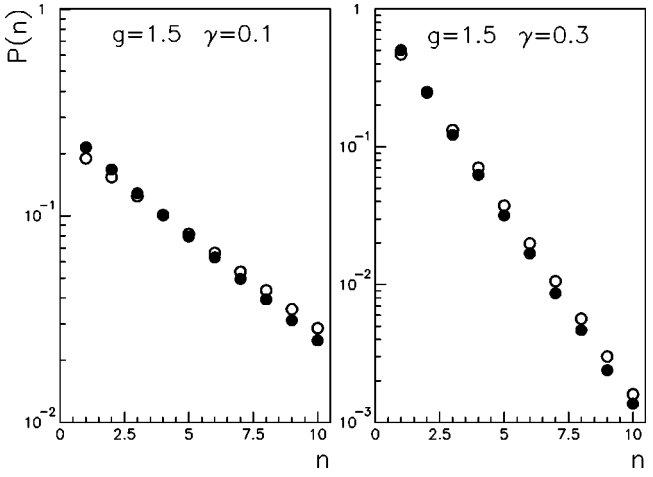

FIG. 4. Jump probabilities at fixed barrier ($g=1.5$, $E_A=6k_BT$) and collision frequency γ. The black circles correspond to the exact numerical data $P(n)$ and the open circles to the analytical result $P^*(n)$. The error bars on the numerical points are smaller than the size of the dots.

In Fig. 4 we report the behavior of $P(n)$ at fixed γ and g for two different γ values. The numerical results are represented by black circles, and the open circles correspond to the $P^*(n)$ [Eqs. (28) and (29)]. The decay with n is very close to an exponential, with small deviations (i.e., a slightly faster decay) at small n. The analytical approximation is very good (and it is exactly exponentially decaying). The deviations from an exponential decay were much more evident in the case of the Fokker-Planck equation [8], and were attributed to the nonequilibrium distribution (at low γ) of the particles coming out from the well of departure. Here, the direct simulation of the model has not revealed any deviation from the Maxwell distribution for the escaping particles.

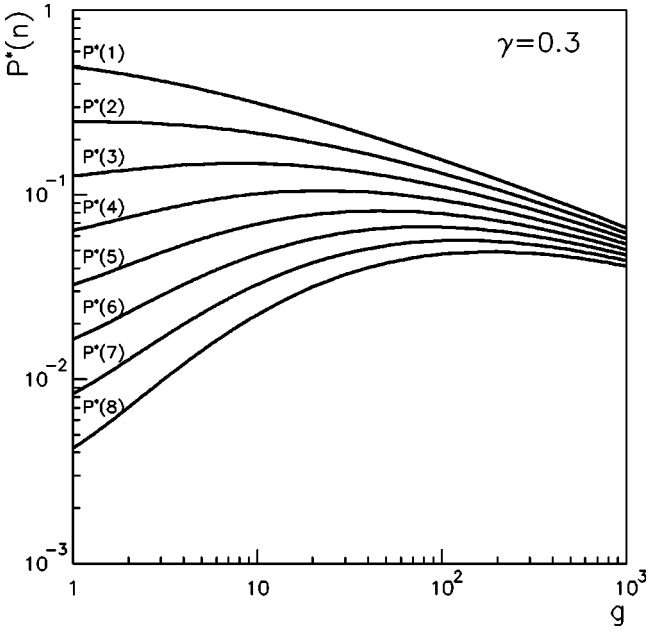

FIG. 5. $P^*(n)$ for $n=1,2,\ldots,8$ as functions of the energy barrier at fixed collision frequency.

Finally, in Fig. 5, the behavior of $P^*(n)$ for $n=1,2,\ldots,8$ is reported as a function of g at fixed γ. Only the analytical results are reported because the numerical solution is not feasible at very large barriers. We tested (up to $g=4$, the highest value at which the numerical calculations require a reasonable effort) that the accuracy of the analytical approximation improves as the activation barrier is raised. We notice that the probability of single jumps $P(1)$ *decreases* when the barrier is raised at fixed η and temperature (i.e., when g is increased keeping γ fixed). Therefore, in the strong-collision model, we have more and more long jumps increasing the barrier height. This is the opposite of what happens in the case of Fokker-Planck [8], and can be understood in the following terms. In the strong-collision model, to the first approximation, the probability of being trapped in the first cell, thus making a single jump, increases with the time spent in the cell, which is given by $\tilde{\varphi}/\eta$ [see Eq. (18)]. This time decreases at larger barriers (if the other parameters are kept fixed) because the velocity $v(x,\varepsilon)$ increases with the barrier: at larger barriers, the particle suffers a stronger acceleration towards the bottom of the well. On the contrary, in the Fokker-Planck case, the probability of being trapped in the first cell increases with the dissipation parameter Δ (see for example [8]) defined as

$$\Delta(\varepsilon)=\frac{\eta}{k_B T}\int_0^a dx\, v(x,\varepsilon) \tag{34}$$

which contains the velocity at the numerator and thus has an opposite behavior at increasing barrier. In fact, in the Fokker-Planck case, due to the frictional force $-\eta v$, a larger velocity causes a larger dissipation and a larger retrapping probability.

V. CONCLUSIONS

In this paper the jump-length probability distribution for a particle diffusing in a periodic potential in the strong-collision model (in which each collision with the thermal bath suddenly thermalizes the velocity) has been calculated with different methods, numerical and analytical. The numerical results have been obtained mainly by the matrix-continued-fraction method, which becomes cumbersome at high barriers and/or low collision frequencies. On the other hand, also the direct simulation of the model can cover only a limited range of parameters with a reasonable computational effort. Because of that, the development of reliable analytical approximations is important. Two different approximations have been proposed. In the first approximation, it has been assumed that all the particle is always trapped in the cell where it suffers its first collision, thus identifying, for a *unbound* particle, the collision frequency and the retrapping frequency. It can be easily understood that this approximation overestimates the percentage of single jumps, as it is confirmed by the comparison with the numerical results. A second (and better) approximation has been obtained with the assumption that only a part of the collisions are effective, i.e., those collisions after which the total energy of the particle lies below the saddle-point energy. This leads to the definition of an effective collision frequency, which is identified with the retrapping frequency. In this case, the results are very close to the exact numerical ones, and the single-jump fraction is underestimated. The fact that the second approximation works better than the first can be understood by noticing that the second approximation treats practically in an exact way what happens at the first collision, whereas the first approximation is not even exact at this stage.

ACKNOWLEDGMENT

The authors acknowledge financial support from the Italian Ministero dell'Università e della Ricerca Scientifica e Tecnologica under the project *Dalle Superfici Ideali a Quelle Reali*.

[1] H. Risken, *The Fokker-Planck Equation* (Springer, Berlin, 1989).
[2] *Noise in Nonlinear Systems*, edited by F. Moss and P.V.E. McClintock (Cambridge University Press, Cambridge, England, 1989).
[3] P. Jung, Phys. Rep. **234**, 175 (1993).
[4] T. Ala-Nissila and S.C. Ying, Prog. Surf. Sci. **39**, 227 (1992).
[5] P.L. Bhatnagar, E.P. Gross, and M. Krook, Phys. Rev. **94**, 511 (1954).
[6] S. Yu. Krylov. A.S. Prosyanov, and J.J.M. Beenhakker, J. Chem. Phys. **107**, 6970 (1997).
[7] D.J. Bicout, A.M. Berezhkovskii, A. Szabo, and G.H. Weiss, Phys. Rev. E **59**, 3702 (1999).
[8] R. Ferrando, R. Spadacini, and G.E. Tommei, Phys. Rev. E **48**, 2437 (1993); Surf. Sci. **265**, 273 (1992); R. Ferrando, R. Spadacini, G.E. Tommei, and G. Caratti, *ibid.* **311**, 411 (1994); G. Caratti, R. Ferrando, R. Spadacini, and G.E. Tommei, Phys. Rev. E **54**, 4708 (1996); Chem. Phys. **234**, 157 (1998).
[9] L.Y. Chen and S.C. Ying, Phys. Rev. Lett. **71**, 4361 (1993); L.Y. Chen, M.R. Baldan, and S.C. Ying, Phys. Rev. B **54**, 8856 (1996).
[10] Yu. Georgievskii and E. Pollak, Phys. Rev. E **49**, 5098 (1994); E. Hershkovitz, P. Talkner, E. Pollak, and Y. Georgievskii, Surf. Sci. **421**, 73 (1999); P. Talkner, E. Hershkovitz, E. Pollak, and P. Hänggi, *ibid.* **437**, 198 (1999).
[11] G. Wahnström, Surf. Sci. **159**, 311 (1985); Phys. Rev. B **33**, 1020 (1985); J. Chem. Phys. **84**, 5931 (1986).
[12] D. Cowell Senft and G. Ehrlich, Phys. Rev. Lett. **74**, 294 (1995).
[13] T.R. Linderoth, S. Horch, E. Laegsgaard, I. Stensgaard, and F. Besenbacher, Phys. Rev. Lett. **78**, 4978 (1997).
[14] V.I. Mel'nikov, Phys. Rep. **209**, 1 (1991).
[15] G.J. Moro and A. Polimeno, Chem. Phys. Lett. **189**, 133 (1992).
[16] P. Jung and B.J. Berne, in *New Trends in Kramers Reaction Rate Theory*, edited by P. Talkner and P. Hanggi (Kluwer Academic, Amsterdam, 1995).
[17] M. Borromeo, G. Costantini, and F. Marchesoni, Phys. Rev. Lett. **82**, 2820 (1999).

[18] A. Asaklil, M. Mazroui, and Y. Boughaleb, Eur. Phys. J. B **10**, 91 (1999).

[19] J.J.M. Beenakker and S.Yu. Krylov, Surf. Sci. **411**, L816 (1998).

[20] R. Ferrando, R. Spadacini, G.E. Tommei, and G. Caratti, Physica A **195**, 506 (1993).

[21] R. Ferrando, R. Spadacini, and G.E. Tommei, Chem. Phys. Lett. **202**, 248 (1993).

[22] D. Frenkel and B. Smit, *Understanding Molecular Simulation* (Academic Press, San Diego, 1996).

[23] L.Y. Chen and S.C. Ying, Phys. Rev. B **60**, 16 965 (1999).